Available online at www.sciencedirect.com
SCIENCE DIRECT®
Journal of Solid State Chemistry 177 (2004) 4640–4647
JOURNAL OF SOLID STATE CHEMISTRY
www.elsevier.com/locate/jssc

One-dimensional shape-controlled preparation of porous Cu_2O nano-whiskers by using CTAB as a template

Ying Yu[a,b], Fei-Peng Du[a], Jimmy C. Yu[c], Yuan-Yi Zhuang[d], Po-Keung Wong[b,*]

[a] *College of Physical Science and Technology, Huazhong Normal University, Wuhan 430079, China*
[b] *Department of Biology, The Chinese University of Hong Kong, Shatin, NT, Hong Kong SAR, China*
[c] *Department of Chemistry, The Chinese University of Hong Kong, Shatin, NT, Hong Kong SAR, China*
[d] *College of Environmental Science and Engineering, Nankai University, Tianjin 300071, China*

Received 26 August 2004; received in revised form 9 October 2004; accepted 13 October 2004
Available online 11 November 2004

Abstract

One-dimensional (1D) cuprite (Cu_2O) nano-whiskers with diameter of 15–30 nm are obtained from liquid deposition method at 25 °C by adding a surfactant, cetyl trimethyl ammonium bromide (CTAB), as a template. TEM and HRTEM show that the nano-whiskers exhibit a well-crystallized 1D structure of more than 200 nm in length, and confirms that the nano-whiskers grow mainly along the $\langle 111 \rangle$ direction. Moreover, there are many pores in the nano-whiskers, which is beneficial for the photocatalysis under visible light. When polyethylene glycol (PEG), glucose and sodium dodecylbenzenesulfonate (SDS) are used as templates, 1D structures cannot be obtained. According to the TEM images of the compound obtained at different stages during the growth of the Cu_2O nano-whiskers, it is found that the role of CTAB is to interact with tiny $Cu(OH)_2$, which can adsorb OH^- and become negative charged, to disperse the tiny $Cu(OH)_2$ solid and to induce the growth of Cu_2O along the 1D direction. Although CTAB is significant for the preparation of the 1D nanomaterials, ion character of the precursor ($Cu(OH)_2 \cdot OH^-$ or Cu^{2+}) is important as well since there is no nano-whiskers obtained with Cu^{2+} as the precursor. Moreover, the probable mechanism of the formation for the porous structure is discussed.

Keywords: 1D nanostructure; Cu_2O; CTAB; Porous structure; Shape and morphology control; SDS; PEG

1. Introduction

Over the past decade, one-dimensional (1D) nano-structures such as nano-tubes [1], inorganic nano-rods and nano-wires [2–4] have attracted considerable attention. Much effort has been directed toward understanding the electronic, magnetic and optical properties of these nano-structures because they show physical and chemical properties different from their bulk counterparts. It has been found that their properties depend largely on their size and shape. So, one of the challenges in nano-crystal synthesis is to control not only the size but the shape and morphology of the crystal [5]. Nano-whiskers are also 1D structure [6] and they offer the possibility to study the physical property of 1D transport, as well as creating new devices based on quantum physics. The growth of semiconductor whiskers is a well-known phenomenon and was thoroughly evaluated in the 1960s [7]. The dimensions of such whiskers have since then been scaled down to reach the quantum regime.

The most widely used method for the fabrication of 1D nano-materials is physical or chemical method guided by an appropriate porous "hard" template and versatile "soft" template such surfactants. The hard template approach is effective, but some of templates are not easy to be fabricated and removed. The application

*Corresponding author. Fax: +852 2603 5767.
E-mail address: pkwong@cuhk.edu.hk (P.-K. Wong).

0022-4596/$ - see front matter © 2004 Elsevier Inc. All rights reserved.
doi:10.1016/j.jssc.2004.10.025

of electrostatic interactions between surfactant molecules and charged or polarized metal-oxyprecursors as the inorganic component has opened a new way to metastable modifications of metal oxides [8]. Cetyltrimethylammonium bromide (CTAB) is a cationic surfactant, which can form CH_3–CH_3–CH_3–N structure and induce the sphere-rod transition of micelles in aqueous solution when some salts such as NaCl, Na_2SO_4 and so on are added [9]. Therefore, CTAB can be employed to synthesize materials with special morphologies. Ag nano-rods [10], Au nano-rods [11], lamellar tin (IV) sulfide [12], SnS nano-wires [13] and hydroxyapatite nano-structure [14] have been prepared with CTAB as a "soft" template.

Cu_2O is a non-stiochoimetric *p*-type semiconductor, which is inexpensive and abundantly available. It has a direct band gap of 2.0 eV [15] and a high optical absorption coefficient, and its theoretical solar cells conversion efficiency is over 13% [16]. It has been used in hydrogen production [17] under visible light, solar cell [18], and negative electrode material for lithium ion batteries [19]. It also has a great potential in photocatalytic degradation of organic pollutants under visible light [20]. Over the past several years, 1D nano-scale Cu_2O has been synthesized by chemical deposition [21], electro-deposition [22,23] and template method [24]. CTAB has been also used as a template to synthesize Cu_2O nano-tubes and nano-rods [25]. However up to now, 1D Cu_2O nano-materials with pores on their surface have not been reported and the effect of different templates and the ion character of the precursor on the formation of 1D nano-Cu_2O have never been studied in details. In this paper, high resolution transmission electron microscopy (HRTEM) analysis is used to analyze the morphology of Cu_2O nano-whiskers with pores prepared in the presence of CTAB as a template. Then, the results are compared with those using polyethylene glycol (PEG), glucose and sodium dodecylbenzenesulfonate (SDS), respectively, as a template. Furthermore, transmission electron microscopy (TEM) images of the compound obtained at different reaction stages during the growth of the nano-whiskers are recorded to explore the controllable role of CTAB on the morphology of Cu_2O nano-materials. To study the importance of the interaction between CTAB and the precursor, the preparation of Cu_2O with NaOH and without NaOH are also carried out.

2. Experimental

All of the chemical reagents used were of analytical grade. The procedure employed for preparing Cu_2O nano-whiskers with CTAB as a template is described by Yu et al. [26]. In a typical synthesis process, 5 g of $CuSO_4 \cdot 5H_2O$ was mixed with 5.5 g of NaOH in 800 ml distilled water. After stirring for 10 min, 20 g of CTAB was added into the stirring solution. After 30 min, 5 ml of 2 M $N_2H_4 \cdot H_2O$ was added dropwise into the mixed solution. The whole reactive system was sealed and flushed with N_2. The colloid gradually formed and turned into a red color. The reaction proceeded for 1.5 or 12 h. The red precipitate was separated with centrifugation, and washed with 200 ml of distilled water, and then 200 ml 95% of ethanol. Finally, it was dried in a vacuum oven at 60 °C for 2 h.

In some experiments, the CTAB template was replaced by PEG ($M_w = 20,000$), glucose or SDS, and the reaction time was 2.5 h. The amount of the three templates added was also the same as that of CTAB. In order to study the effect of precursors (Cu^{2+} and $Cu(OH)_2 \cdot OH^-$ in this case) on the morphology of Cu_2O with CTAB as a template, the similar reaction was also conducted without NaOH. The reaction time was also 2.5 h.

The crystal structure and composition of Cu_2O nano-whiskers were analyzed by X-ray powder diffraction (XRD) using a Brucker Y-2000 X-ray diffractometer with Cu$K\alpha$ radiation ($\lambda = 0.154178$ nm) at 25 °C. A scan rate of 0.03°/s was applied to record the powder patterns for 2θ between $20° \leqslant 2\theta \leqslant 80°$. Powder morphology, size and selected area electron diffraction (SAED) were characterized by TEM by a JEM-100CXV transmission electron microscope using an accelerating voltage of 80 kV. HRTEM images were obtained by a JEOL JEM 2010FEF electron microscope using an accelerating voltage of 200 kV. Brunauer–Emmett–Teller (BET) surface areas of the samples were determined using a Micromeritics ASAP 2010 nitrogen adsorption apparatus. Before actual measurement, the sample was degassed at 25 °C for 4 h.

3. Results and discussion

3.1. Evolution of Cu_2O nano-whiskers

$N_2H_4 \cdot H_2O$ is chosen as a reducing agent. It oxidizes to an inert gas N_2, which can protect Cu_2O nano-whiskers from oxidation. The formation of Cu_2O can be expressed by the following reactions (Eqs. (1) and (2)):

$$Cu^{2+} + 4OH^- \rightarrow [Cu(OH)_4]^{2-}, \quad (1)$$

$$12H^+ + 4[Cu(OH)_4]^{2-} + N_2H_4 \rightarrow 4Cu^+ + N_2 \uparrow + 16H_2O. \quad (2)$$

Then, Cu^+ may take part in the following two reactions (Eqs. (3) and (4)):

$$4Cu^+ + 4OH^- + N_2H_4 \rightarrow N_2 \uparrow + 4H_2O + 4Cu^0, \quad (3)$$

$$2Cu^+ \rightarrow Cu^{2+} + Cu^0. \quad (4)$$

But in the alkaline solution and by controlling the amount of $N_2H_4 \cdot H_2O$ (mole ratio of $N_2H_4 \cdot H_2O$ and $Cu^{2+} \approx 0.5$), the following reaction (Eq. (5)) dominates.

$$2Cu^{+} + 2\ OH^{-} \rightarrow 2CuOH \rightarrow Cu_2O + H_2O. \quad (5)$$

Once the mole mass of $N_2H_4 \cdot H_2O$ is 3 times more than that of Cu^{2+}, metal copper can be formed [25].

With CTAB, PEG, or SDS as a template, Eq. (5) dominates and leads to Cu_2O formation. With glucose as a template, both glucose and $N_2H_4 \cdot H_2O$ can reduce Cu^{2+} to Cu_2O. The reaction for glucose as a reactant is

$$2Cu(OH)_2 + C_5H_{11}O_5{-}CHO \rightarrow Cu_2O + C_5H_{11}O_5COOH + 2H_2O. \quad (6)$$

Therefore, no matter which template is used, pure Cu_2O can be obtained. Fig. 1 is the XRD analysis of Cu_2O nano-whiskers prepared with CTAB as a template, which shows that there are six peaks with 2θ values of 29.60, 36.52, 42.44, 61.54, 73.69, and 77.74, corresponding to $\langle 110 \rangle$, $\langle 111 \rangle$, $\langle 200 \rangle$, $\langle 220 \rangle$, $\langle 311 \rangle$, and $\langle 222 \rangle$ crystal planes of pure Cu_2O, respectively. These results are in good agreement with the Cu_2O powder obtained from the International Center of Diffraction Data Card reflections (JCPDS, 05–667 and JCPDS, 05–661). The calculated crystalline cell constants is $a = 0.4258$ nm, which is similar to the lattice parameter for the unit cell of the cubic crystal composed of four copper (Cu^{+}) and five oxygen (O^{2-}) ions. The $\langle 111 \rangle$ reflection of the samples obtained is comparatively strong, which is probably due to the orientation of the nano-crystallines.

The TEM and HRTEM images of the Cu_2O nano-whiskers obtained with CTAB as a template are shown in Fig. 2. The morphology of 1D nano-Cu_2O is whiskers-like. The length is more than 200 nm and the diameter is in the range of 15–30 nm (Figs. 2a and b). Moreover, there are many pores in the whiskers as indicated by the arrows in Fig. 2b. Fig. 2c is a representative HRTEM image of Cu_2O crystalline,

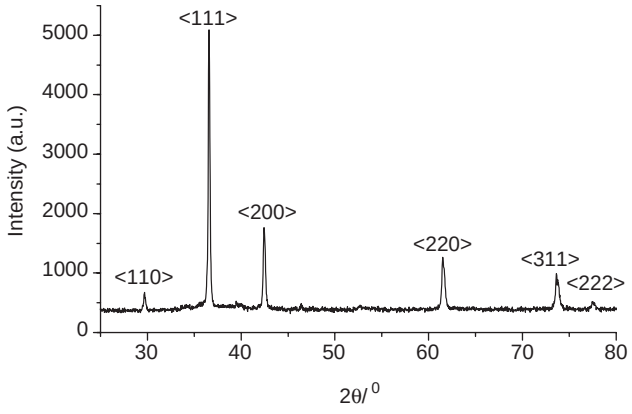

Fig. 1. XRD pattern of Cu_2O nano-whiskers prepared in the presence of CTAB at 25 °C.

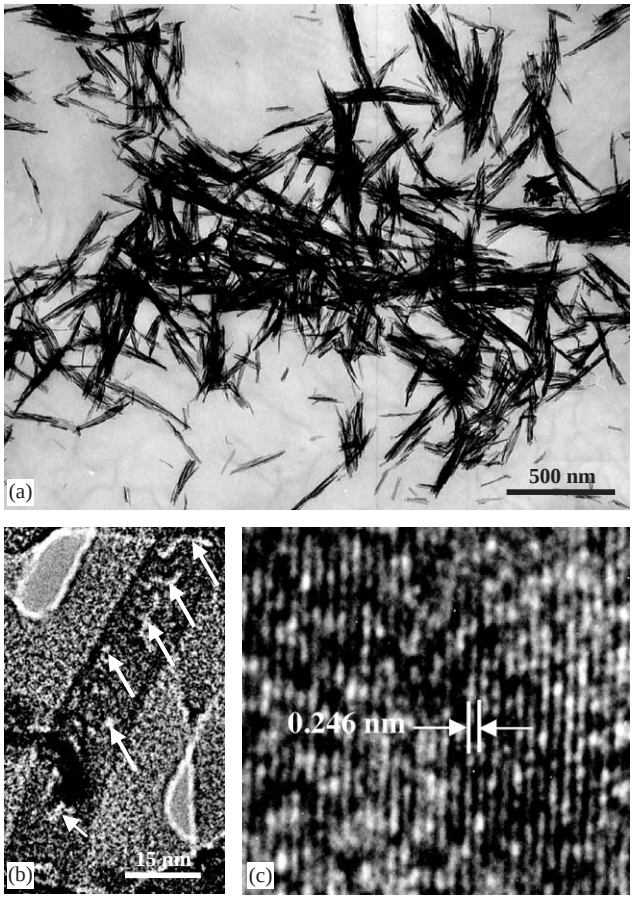

Fig. 2. TEM and HRTEM images of the as-prepared Cu_2O nano-whiskers: (a) and (b) TEM images of the sample collected after 1.5 h reaction time with CTAB as a template, white arrow labels the pores in a piece of nano-whisker, and (c) HRTEM image of the same sample.

which shows the clearly resolved interplanar distance $d_{111} = 0.246$ nm and further confirms that the Cu_2O nano-whiskers grow mainly along the $\langle 111 \rangle$ direction.

In order to confirm the presence of the porous structure in Cu_2O nano-whiskers, BET experiment is conducted. The result is that the BET surface area (S_{BET}) of the whiskers is 42 m^2/g, which is larger than the theoretical value of 33 m^2/g for pure Cu_2O nano-wires. The Barrett–Joyner–Halenda (BJH) pore size distribution plot for N_2-sorption isothermals of the 1D nano-materials is shown in Fig. 3. It can be seen that the main pore size distribution is located at about 3.2 and 33 nm. The main pore of 3.2 nm is attributed to the small mesopore on the surface of the nano-whiskers [27], which has a narrow size distribution. The average pore size basically corresponds to that shown in Fig. 2b. The main pore of 33 nm is the large mesopore between nano-whiskers, which has a broad distribution. Generally speaking, the proportion of the pore on the surface of the nano-whiskers is lower so that the pore between nano-whiskers is dominant and the S_{BET} is not much larger. However, the Cu_2O nano-whiskers will have a

higher adsorption capacity due to the presence of small mesopore on their surface, leading to its good photocatalytic ability under visible light.

3.2. The shape control with CTAB as a template

Fig. 4 shows the TEM images and the corresponding SAED pattern of the Cu_2O obtained under different experimental conditions. Fig. 4a shows the image of the sample prepared without CTAB. The particles grow up and form hexagon and quadrangular crystallines with diameters of 500 nm to 1 μm. Fig. 4b is the image of the sample collected at the reaction time of 12 h with CTAB as a template. The TEM image of the sample collected at 1.5 h is shown in Fig. 2a. It can be seen that the nano-whiskers obtained at 1.5 h are in a uniform diameter (Fig. 2a). However, with the increase of reaction time (i.e., 12 h), most of the whiskers are linked together (Fig. 4b). The corresponding SAED pattern in the Fig. 4c shows that there are some transparent homocentric annuli, which indicate that the sample in Fig. 4b is totally polycrystalline due to the agglomeration of the nano-whiskers.

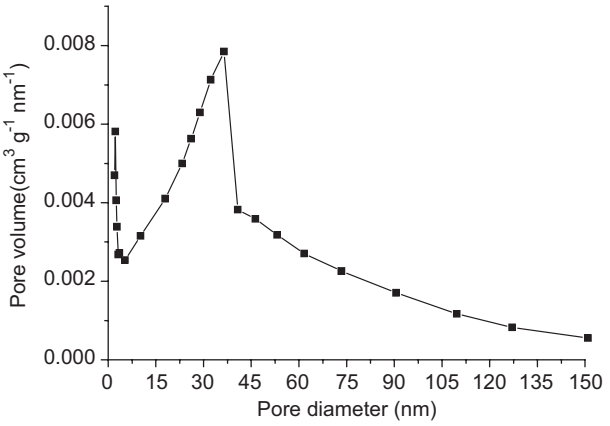

Fig. 3. BJH pore size distribution curve of the as-prepared Cu_2O nano-whiskers.

In order to explore the shape control mechanism of CTAB in the growth of Cu_2O nano-whiskers, the morphology of the compound at different stage in the growing process of Cu_2O nano-whiskers is monitored by TEM analysis (Fig. 5). At the beginning, $Cu(OH)_2$ suspension is formed by the reaction of $CuSO_4$ and NaOH. The morphology of $Cu(OH)_2$ is tiny needles with the length and diameter about 80 and 10 nm, respectively. These tiny needles are twisted with each other (Fig. 5a). When CTAB is added, the twisted needles disappear, while many spherical colloids are formed and many white tiny particles appear on the surface of the spherical colloids (Fig. 5b). After stirring for 30 min, the morphology of nano-rods (Fig. 5c) is observed. With continuous stirring for 1.5 h, Cu_2O nano-whiskers are obtained (Fig. 2a).

Based on the results mentioned above, we propose the following mechanism of the shape control of Cu_2O nano-whiskers by CTAB (Fig. 6). Firstly, the $Cu(OH)_2$ suspension forms tiny amorphous needles because there

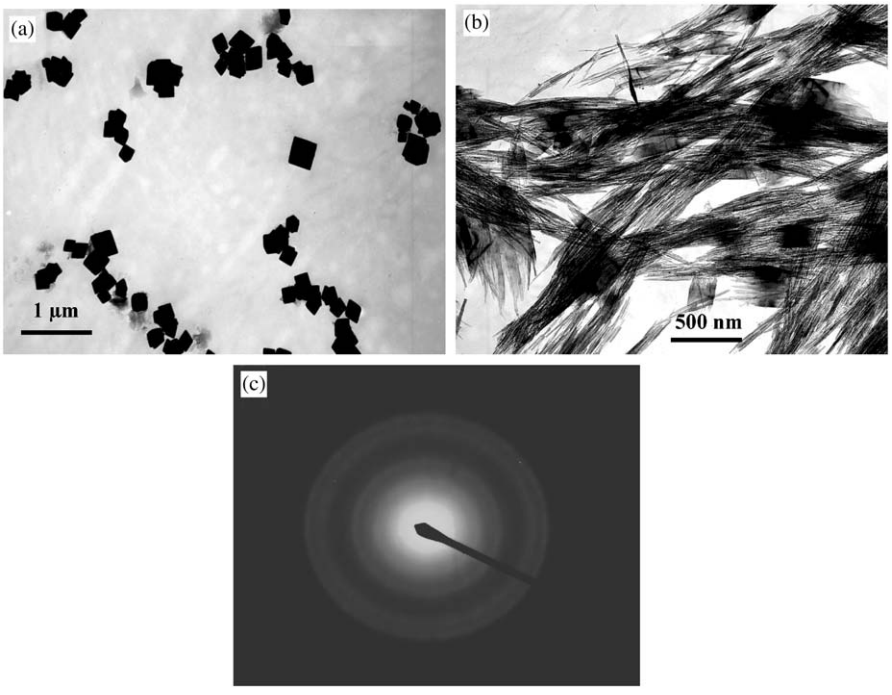

Fig. 4. TEM images and SAED pattern of the various forms of Cu_2O prepared under different experimental conditions: (a) the sample prepared without CTAB, (b) the sample collected after 12 h reaction time with CTAB as a template and (c) SAED pattern of Fig. 4b.

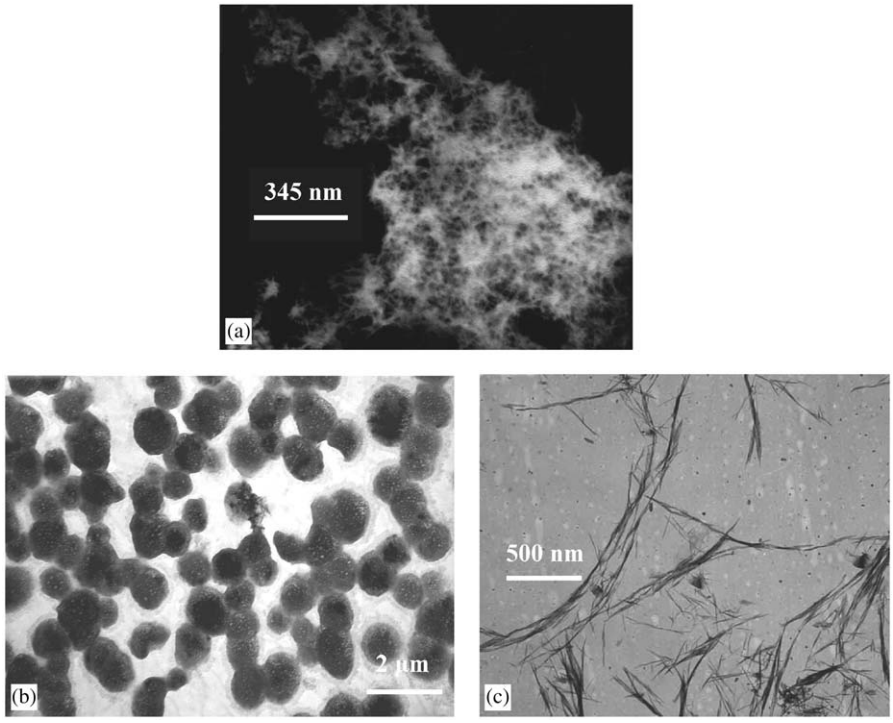

Fig. 5. TEM images obtained in different stages of the reaction process: (a) $Cu(OH)_2$ suspension, (b) the mixture of $Cu(OH)_2$ and CTAB after CTAB is added for 2 min; and (c) the mixture of $Cu(OH)_2$ and CTAB after stirring for 30 min.

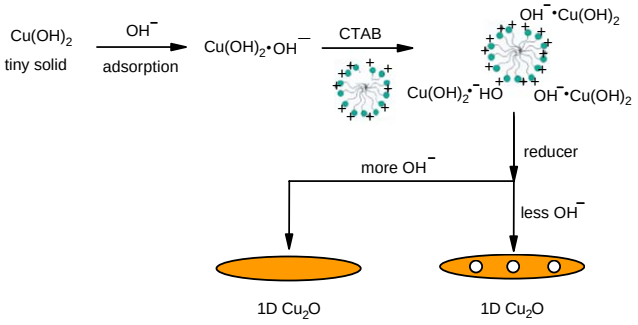

Fig. 6. The scheme for the formation of Cu_2O nano-whiskers and porous structure. Tiny $Cu(OH)_2$ solid adsorbs OH^- and become negatively charged. Then, $Cu(OH)_2 \cdot OH^-$ binds to the cationic CTAN micelles, displace Br^- and the assembled $Cu(OH)_2$ tiny needles are dispersed. After a suitable amount of reducer, $N_2H_4 \cdot H_2O$, is added, 1D Cu_2O is formed due to the existence of CTAB. When less OH^- is present in the system, CTAB can assemble on the interface that Cu_2O grows and inhibits the growth of Cu_2O along the region that CTAB occupied. This results in the formation of pores in the 1D nanomaterials. In the presence of high concentration of OH^-, CTAB cannot assemble on the interface due to excess OH^- can reduce the interaction between $Cu(OH)_2 \cdot OH^-$ and CTAB. Thus, porous structure is not formed.

is no peak in XRD pattern of the according solid. Since the amount of NaOH is about 6 times more than that of Cu^{2+}, $Cu(OH)_2$ is surrounded by OH^-, leading to the adsorption of OH^- onto the surface of $Cu(OH)_2$, and resulting in $Cu(OH)_2$ negative charged and the formation of $Cu(OH)_2 \cdot OH^-$ precursor. Secondly, when cationic CTAB is added, it interacts with the negatively charged $Cu(OH)_2 \cdot OH^-$ through electrostatic interactions to form the inorganic-surfactant composites, in which CTAB serves as a template. The $Cu(OH)_2 \cdot OH^-$ interact electrostatically with the surfactant cationic head groups, CTA^+, to form CTA^+-$Cu(OH)_2 \cdot OH^-$ ion pairs [11]. It seems that CTAB wraps the tiny needles and become spherical micelles when CTAB is added and is not dispersed evenly in the solution (Fig. 5b). The tiny white dots surrounded by the colloid is $Cu(OH)_2$. Thus, assembled $Cu(OH)_2$ is dispersed. Thirdly, for the control of 1D morphology, there are two mechanisms, which may be used for explanation. The first one is that when the ratio between water and CTAB is in a range of 7:3–3:7, middle phase, that is, long cylindrical micelles can be formed [28,29]. Under the reaction conditions, the concentration of CTAB is less than the critical concentration for the rod-shaped micelles. However, due to the property of the easy formation of rod-shaped micelles for CTAB and the interaction of CTAB and $Cu(OH)_2 \cdot OH^-$ [30], the possibility of the vertical diffusion of $Cu(OH)_2$ is reduced. $Cu(OH)_2$ in the micelles tends to diffuse along parallel direction and may be apt to agglomerate at the tip of the crystals [11], resulting in the growth of Cu_2O along 1D direction induced by CTAB when $N_2H_4 \cdot H_2O$ is added. The second mechanism is that, due to the interaction between CTAB and $Cu(OH)_2 \cdot OH^-$, it is possible that

CTAB referentially adsorb some planes of growing Cu_2O with the presence of $N_2H_4 \cdot H_2O$, leading to the growth of Cu_2O along 1D direction. Based on the results and discussion above, it can be concluded that CTAB is significant for 1D Cu_2O nano-structure preparation. In the presence of CTAB, assembled $Cu(OH)_2$ is dispersed and nucleates at the micelles. Then, Cu_2O has a high probability to grow along 1D direction induced by CTAB.

With the increase of the reaction time, $Cu(OH)_2$ in the layers of CTAB is converted to Cu_2O. The ion pairs CTA^+-$Cu(OH)_2 \cdot OH^-$ disappear. Owing to the large surface area of Cu_2O nano-whiskers, they are easy to link with each other. Therefore, after the reaction proceeding for 12 h, the size of the obtained Cu_2O whiskers becomes much larger (Fig. 4b).

Compared with the experimental conditions for the preparation of 1D Cu_2O nano-materials of the previous study [25], the amount of NaOH may be crucial for the formation of porous structure since the concentration of CTAB is the same for the previous study and this study. In the previous study, the molar ratio of Cu^{2+} and NaOH is 1:200, while in this study, the molar ratio of Cu^{2+} and NaOH is 1:7. Thus, less NaOH may be beneficial for the pore formation. The mechanism for the pore formation is still unclear and need further study. Based on the results obtained in this study, a speculation is proposed and the scheme is shown in Fig. 6. During the crystal growth, defect generation is a normal phenomenon [31]. Since CTAB interacts with $Cu(OH)_2 \cdot OH^-$, it is possible that CTAB is present at the interface that Cu_2O crystal grows. Thus, the surfactant may assemble in the interface region and inhibit the growth of Cu_2O around the region of the assembled CTAB [32]. Therefore, the region with CTAB is left in the solid as the interface advances. Thus, defects are formed. After the samples are washed or irradiated by high-energy electron beam of TEM, CTAB is released or evaporated and pores are left. When a large amount of OH^- are present in the system, excess OH^- can shield the interaction between CTAB and $Cu(OH)_2 \cdot OH^-$ so that the interaction decrease. OH^- is a small ion and cannot greatly increase the distance of the interaction so that CTAB can still affect the growth dimension of Cu_2O crystal. However, the possibility to assemble in the interface region is hardly present. Thus, there is no pore on 1D Cu_2O nano-materials in the previous study in the presence of high concentration of OH^-. In this study, the concentration of OH^- is comparably less, and its effect is too small to reduce the interaction of CTAB and $Cu(OH)_2 \cdot OH^-$. Thus, porous structure is formed.

3.3. Comparison of CTAB with other templates

Fig. 7 shows the TEM images of the Cu_2O obtained with glucose, SDS or PEG as a template. Brick red crystals can also be obtained in the presence of these templates. However, the size and the morphology of Cu_2O nano-crystals are different from those formed with CTAB as a template. Needle-like nano-size Cu_2O and bulk Cu_2O can be both observed when glucose as a template in the preparation. It indicates that the tiny Cu_2O is easy to assemble (Fig. 7a). With anionic

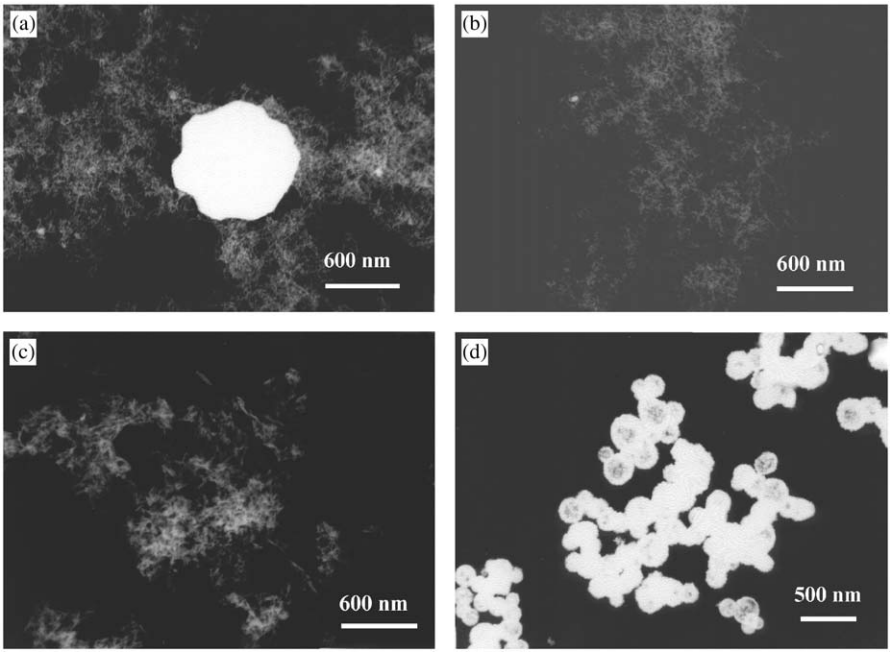

Fig. 7. TEM images for the Cu_2O obtained with different templates. (a) glucose, (b) SDS, (c) PEG, and (d) CTAB without NaOH.

surfactant SDS and nonionic surfactant PEG as a template, needle-like Cu_2O is also obtained but the size of the needles with SDS as a template is smaller and the dispersion is more evenly (Fig. 7b). The Cu_2O prepared with PEG as a template is interlaced with each other (Fig. 7c). With the three organic templates, nano-Cu_2O is synthesized and the morphology is similar to that of $Cu(OH)_2$ suspension. So, the pre-existing $Cu(OH)_2$ suspension provides the nucleation sites for Cu_2O crystal and has an effect on the growth direction for Cu_2O [33]. Because there is no strong interaction between $Cu(OH)_2$ suspension and the three templates and there is no possible rod-shaped micelles formed in the presence of SDS and PEG. Cu_2O crystal grows according to the nucleation sites provided by $Cu(OH)_2$ and results in the tiny needle-like morphology. Glucose is not a surfactant and it cannot disperse particles. Therefore, the tiny crystals would agglomerate to form bulk Cu_2O. SDS and PEG are both surfactants so that the crystalline products are comparatively dispersed. SDS is small molecule surfactant and the micelles formed by SDS are also small. It can disperse $Cu(OH)_2$ suspension into more tiny colloid so that the finally obtained crystals are the smallest. PEG is polymer surfactant and its micelles are big, leading to the formation of biggest crystals. Owing to the twisted property of polymeric segments, the whiskers are also interlaced with each other.

3.4. Effect of the ionic nature of the precursor

When NaOH is present, $Cu(OH)_2 \cdot OH^-$ is the precursor and Cu_2O nano-whiskers can prepared. Without NaOH, Cu^{2+} is the precursor and Cu_2O can be produced as well. The reaction is as follows:

$$4Cu^{2+} + NH_2 \cdot NH_2 \rightarrow 4Cu^{+} + N_2 \uparrow + 4H^{+}. \quad (7)$$

However, the morphology of the obtained Cu_2O is quite different from that with $Cu(OH)_2 \cdot OH^-$ as a precursor. It becomes spherical with a diameter about 200 nm and some of them are hollow in the middle (Fig. 7d). It is a interesting phenomenon because such kind of spherical hollow Cu_2O has been reported with NaOH and $Cu(CH_3COO)_2$ as reactants [34]. The 1D nano-structure cannot be obtained because the interaction between copper ion and CTAB does not exist so that the growth of Cu_2O crystal cannot be affected by CTAB. Meanwhile, CTAB is easy to adsorb onto the clusters to form surface ion-pairs [11]. Without NaOH in the system, there is no $Cu(OH)_2 \cdot OH^-$ clusters so that Cu^{2+} grows freely and leads to the formation of spherical crystals. For the growth mechanism of the spherical hollow Cu_2O, further study is required. These results suggest ionic character of the precursor is also important to control the morphology of Cu_2O nano-whiskers.

4. Conclusions

With the cationic surfactant CTAB as a template, 1D Cu_2O nano-structure can be obtained. The nano-whiskers are highly porous, which will be beneficial for the photocatalytic activity under visible light. According to the TEM images of the morphology of the compounds at the different growth stages and the comparison of the result obtained with and without NaOH, it can be confirmed that there is electrostatic interaction between the precursor $Cu(OH)_2 \cdot OH^-$ suspension and CTAB. Moreover, CTAB can induce Cu_2O to grow along 1D direction since nano-whiskers cannot be synthesized with other surfactants as templates. Although CTAB is important to control the morphology of 1D nano-materials, ion character of the precursor is also significant for this aspect.

Acknowledgments

The work is supported by a grant from Research Grants Council of the Hong Kong SAR Government, China to P.K. Wong (Project No. CUHK4325/03M) and the National Natural Science Foundation of China to Y. Yu (Project No. 20207002).

References

[1] W. Liang, M. Bockrath, D. Bozovic, J.H. Hafner, M. Tinkham, H. Park, Nature 411 (2001) 665.
[2] J. Yu, J.C. Yu, W. Ho, L. Wu, X. Wang, J. Am. Chem. Soc. 126 (2004) 3422.
[3] S.S. Chang, C.W. Shih, C.D. Chen, W.C. Lai, C.R.C. Wang, Langmuir 15 (1999) 701.
[4] Y. Lei, L.D. Zhang, J.C. Fan, Chem. Phys. Lett. 338 (2001) 231.
[5] J.J. Shiang, A.V. Kadavanich, R.K. Grubbs, A.P. Alivisatos, J. Phys. Chem. 99 (1995) 17417.
[6] B.J. Ohlsson, M.T. Björk, A.I. Persson, C. Thelander, L.R. Wallenberg, M.H. Magnusson, K. Deppert, L. Samuelson, Physica E 13 (2002) 1126.
[7] R.S. Wagner, A.P. Levitt (Eds.), Whisker Technology, Wiley Press, New York, 1970, pp. 47–119.
[8] Q. Huo, D.I. Margolese, U. Cielsa, P. Feng, T.E. Gier, P. Sieger, R. Leon, P.M. Petroff, F. Schüth, G.D. Stucky, Nature 368 (1994) 317.
[9] R. Zielinski, S. Ikeda, H. Nomura, S. Kato, J. Colloid Int. Sci. 125 (1988) 497.
[10] N.R. Jana, L. Gearheart, C.J. Murphy, Chem. Commun. (2001) 617.
[11] J. Perez-Juste, L.M. Liz-Marzan, S. Carnie, D.Y.C. Chan, P. Mulvaney, Adv. Funct. Mater. 14 (2004) 571.
[12] J. Li, L. Delmotte, H. Kessler, Chem. Commun. (1996) 1023.
[13] Y. Liu, D. Hou, G. Wang, Chem. Phys. Lett. 379 (2003) 67.
[14] J. Yao, W. Tjandra, Y.Z. Chen, K.C. Tam, J. Ma, B. Soh, J. Mater. Chem. 13 (2003) 3053.
[15] C. Kittel, Introduction to Solid State Physics, Wiley, New York, 1986.
[16] D.A. Tryk, A. Fujishima, K. Honda, Electrochim. Acta 45 (2000) 2363.

[17] T. Takata, S. Ikeda, A. Tanaks, S. Hara, J.N. Kondo, K. Domen, Appl. Cata. A: Gen. 200 (2000) 255.
[18] B.P. Rai, Phys. Status Solidi A 99 (1987) k35.
[19] P. Poizot, S. Laruelle, S. Grugeon, L. Dupont, J.-M. Taracon, Nature 407 (2000) 496.
[20] J. Ramírez-Ortiz, T. Ogura, J. Medina-Valtierra, S.E. Acosta-Ortiz, P. Bosch, J.A. de los Reyes, V.H. Lara, Appl. Surf. Sci. 174 (2001) 177.
[21] W.Z. Wang, G.H. Wang, X.S. Wang, Adv. Mater. 14 (2002) 67.
[22] L. Huang, H. Wang, Z. Wang, Chem. Mater. 14 (2002) 876.
[23] J. Oh, Y. Tak, Y. Lee, Electrochem. Solid State 7 (2004) C27.
[24] W.Z. Wang, O.K. Varghese, C.M. Ruan, M. Paulose, C.A. Grimes, J. Mater. Res. 18 (2003) 2756.
[25] M. Cao, C. Hu, Y. Wang, Y. Guo, C. Guo, E. Wang, Chem. Commun. (2003) 1884.
[26] Y. Yu, F.P. Du, S.J. Yang, J.L. Li, CN. Pat. Appl. No. 03128315.2.
[27] S.A. Walker, J.A. Zasadzinski, in: S. Komarneni, D.M. Smith, J.S. Beck (Eds.), Advances in Porous Materials, Materials Research Society, Pittsburgh, PA, 1995, p. 93.
[28] S.I. Ahmad, S. Friberg, J. Am. Chem. Soc. 95 (1973) 5196.
[29] L. Yan, Y.D. Li, Z.X. Deng, J. Zhuang, X.M. Sun, Int. J. Inorg. Mater. 3 (2000) 633.
[30] Y. Xiong, Y. Xie, G. Du, X. Tian, J. Mater. Chem. 12 (2002) 98.
[31] R. Philips, Crystals, Defects and Microstructures: Modeling Across Scales, Cambridge University Press, Cambridge, 2001, p. 311.
[32] W.A. Tiller, The Science of Crystallization: Macroscopic Phenomena and Defect Generation, Cambridge University Press, Cambridge, 1991, p. 418.
[33] R.I. Nooney, D. Thirunavukkarasu, Y. Chen, R. Josephs, A.E. Ostafin, Langmuir 19 (2003) 7628.
[34] M. Yang, J.J. Zhu, J. Crystal Growth 256 (2003) 134.